DALTON
FULL PAPER

# Reduction of the anti-cancer drug analogue *cis*,*trans*,*cis*-$[PtCl_2(OCOCH_3)_2(NH_3)_2]$ by L-cysteine and L-methionine and its crystal structure †

**Lie Chen, Peng Foo Lee, John D. Ranford,* Jagadese J. Vittal and Siew Ying Wong**

*Department of Chemistry, National University of Singapore, Lower Kent Ridge Road, 119270 Singapore. E-mail: chmjdr@nus.edu.sg*

***Received 15th January 1999, Accepted 3rd March 1999***

The complex *cis*,*trans*,*cis*-$[PtCl_2(OCOCH_3)_2(NH_3)_2]$ **1** has been synthesized as a simplified and more soluble model of the anticancer drug *cis*,*trans*,*cis*-$[PtCl_2(OCOCH_3)_2(NH_3)(C_6H_{11}NH_2)]$ (JM216). The crystal structure of **1** shows an octahedral co-ordination sphere around the $Pt^{IV}$ with strong intramolecular and weak intermolecular hydrogen bonding. The kinetics of reduction of **1** by the divalent sulfur amino acids L-cysteine and L-methionine has been determined over a range of pH values by multinuclear NMR. The reduction is strongly pH dependent, being related to the protonation state of the amino acid and the basicity of the sulfur. Reduction rates are dramatically slower than for previous models of platinum(IV) drug systems.

Cisplatin, *cis*-diamminedichloroplatinum(II), is an anticancer drug widely used to treat a variety of tumours, especially those of the testes, ovaries, head, and neck.[1] Its intensive use has been restricted by several drawbacks such as side-effects, the development of resistance during therapy and the need for intravenous administration.[2] This has therefore been the impetus for a world-wide search for new platinum-containing drugs. The efforts have resulted in the development of "second-generation" cisplatin analogues, such as carboplatin [diammine(cyclobutane-1,1-dicarboxylato)platinum(II)], and "third generation" analogues, *e.g.* *cis*,*trans*,*cis*-$[PtCl_2(OCOCH_3)_2(NH_3)(C_6H_{11}NH_2)]$ [**2**, JM216; bis(acetato)amminedichloro(cyclohexylamine)platinum(IV)].[3]

Platinum(IV) complexes undergo ligand substitution reactions much more slowly than their platinum(II) analogues, and are therefore usually seen as prodrugs for platinum(II) compounds. Currently the compounds tetraplatin [tetrachloro(1,2-diaminocyclohexane)platinum(IV)], iproplatin [*cis*,*trans*,*cis*-dichlorodihydroxobis(isopropylamine)platinum(IV)] and JM216 are undergoing clinical trials[4] with the latter being the first orally administered platinum complex.[5]

The platinum(IV) species is supposedly activated by reduction to its platinum(II) analogue before hydrolysis and substitution reactions can occur.[6] Thiol and thioether containing biomolecules and ascorbic acid have been proposed as the major cellular components responsible for that reduction.[7] Therefore L-cysteine (L-$H_2$cys) and L-methionine (L-Hmet), either as free amino acids or as components of intracellular peptides and proteins, are considered to be potential reductants for $Pt^{IV}$. Studies on the platinum(IV) complexes *trans*-$[Pt(CN)_4X_2]^{2-}$ (where X is $Cl^-$ or $Br^-$) as stable models for anticancer drugs with L-Hmet[8] and four thiols[7] including L-$H_2$cys have been conducted. Stop-flow techniques had to be employed because of the rapid reactions. The reactions are pH dependent and for the thiols were limited to pH values below 5 because of this. The proposed mechanism involves association of the reductant through the chloro ligands in a transition state and subsequent electron transfer.

† *Supplementary data available*: $^{15}$N NMR spectra of **1** with L-cysteine. Available from BLDSC (No. SUP 57512, 2 pp.). See instructions for Authors, 1999, Issue 1 (http://www.rsc.org/dalton).

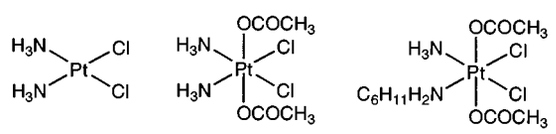


Cisplatin **1** **2** (JM216)

In the present study, we use *cis*,*trans*,*cis*-$[PtCl_2(OCOCH_3)_2(NH_3)_2]$ **1** as a simplified model of **2**, as its aqueous solubility is significantly higher than that of **2**, its synthesis more straightforward, especially for incorporation of $^{15}$N labels, and it eliminates possible isomerism in reaction products due to the inequivalent amines in **2**. We report here the crystal structure and characterization of **1** and kinetic studies of its reduction by the sulfur containing amino acids L-$H_2$cys and L-Hmet using multinuclear NMR.

## Experimental

### Preparations

Cisplatin was synthesized following the method of Dhara[9] and *cis*,*trans*,*cis*-$[PtCl_2(OH)_2(NH_3)_2]$ **3** was prepared by oxidation of cisplatin with $H_2O_2$.[10] $^{15}$N-Enriched complex **1** was synthesized using *cis*-$[PtCl_2(^{15}NH_3)_2]$ prepared from $^{15}NH_4Cl$.

***cis*,*trans*,*cis*-$[PtCl_2(OCOCH_3)_2(NH_3)_2]$ 1.** This was synthesized by carboxylation of its hydroxide analogue **3** with acetic anhydride. A solution of **3** (0.830 g, 2.49 mmol) was stirred in acetic anhydride (20 $cm^3$, 0.212 mol) for 2 h. The product was precipitated with hexane and the solution cooled at 0 °C for 24 h. The solid was filtered off and washed with ethanol, diethyl ether and dried *in vacuo*. Yield: 0.60 g (60%) (Found: C, 11.64; H, 2.94; N, 6.65. Calc. for $C_4H_{12}Cl_2N_2O_4Pt$: C, 11.48; H, 2.87; N, 6.70%). $^1$H NMR ($D_2O$): $\delta$ 2.10 (s).

### NMR spectroscopy

The NMR spectra were recorded on Bruker ACF300 ($^1$H 300 MHz) and AMX500 ($^{15}$N 50.70 MHz) spectrometers using 5 mm NMR tubes. The chemical shift references were as follows: (internal) $^1$H, 4,4-dimethyl-4-silapentane-1-sulfonate, DSS; $^{15}$N, 1.5 M $^{15}NH_4Cl$ in 1 M HCl containing 10% $D_2O$ in a capillary. Samples for $^1$H NMR were made up in deuteriated phosphate

buffer (0.1 M, pH* 7.0) which was prepared by freeze-drying solutions in water and redissolving in $D_2O$, with pH* readjustment as necessary; pH* refers to the pH meter reading in $D_2O$ solution. Samples for $^{15}N$ NMR were prepared in 90% water–10% $D_2O$ phosphate buffer.

### Solubility determination

Samples were suspended in water then ultrasonicated for 2 min. The excess of solid was filtered off, the volume of supernatant was measured prior to lyophilization, then the solid was weighed.

### Cyclic voltammetry

The cyclic voltammetry was performed in a BAS 100B (Bioanalytical Systems Inc.) cell. The electrodes were: working, glassy carbon; counter, platinum foil; reference Ag–AgCl–Cl. All solutions were degassed by bubbling with $N_2$ before measurements.

### Crystallography

**Crystal data.** $C_4H_{14}Cl_2N_2O_5Pt$ **1**, $M = 436.16$, monoclinic, space group $C2/c$, $a$ 14.9973(3), $b$ 8.57220(10), $c$ 11.1352(2) Å, $\beta$ 126.7690(10)°, $U = 1146.74(3)$ Å$^3$, $\lambda = 0.71073$ Å, $Z = 4$, $D_c = 2.526$ Mg m$^{-3}$, $\mu$(Mo-K$\alpha$) 12.701 mm$^{-1}$, 293 K, crystal dimensions 0.38 × 0.32 × 0.27 mm.

**Data collection and structural analysis.** Data were collected on a Siemens SMART CCD diffractometer with the crystal sealed in a glass capillary tube. Preliminary cell constants were obtained from 45 frames of data (width 0.3° in $\omega$). Final cell parameters were obtained by global refinements of reflections obtained from integration of all the frame data. A total of 3597 reflections were collected in the $\theta$ range 2.92–29.07° ($-20 \le h \le 19$, $-11 \le k \le 5$, $-14 \le l \le 13$), 1421 independent reflections ($R_{int}$ 0.0547) with a frame width of 0.3° in $\omega$ and a counting time of 20 s per frame. The collected frames were integrated using the preliminary cell-orientation matrix. The software SMART[11] was used for collecting frames of data, indexing reflections and determination of lattice parameters, SAINT for integration of reflection intensity and scaling, SADABS[12] for absorption correction and SHELXTL[13] for space group and structure determination, refinements (full-matrix least squares on $F^2$), graphics and structure reporting. All the non-hydrogen atoms in the molecules were refined anisotropically. The hydrogen atoms were placed in the ideal positions using riding models. Maximum and minimum transmission 0.1159 and 0.0305 respectively with goodness of fit on $F^2$ 1.114 and extinction coefficient 0.0062(5). Final $R$ indices [$I > 2\sigma(I)$] were $R1$ 0.0386, $wR2$ 0.0965 for the 70 parameters refined. The corresponding values for all data after merging were $R1$ 0.0391 and $wR2$ 0.0967 respectively; $F(000)$ 816. The largest difference peak 2.226 and hole −2.765 e Å$^{-3}$ were associated with Pt.

CCDC reference number 186/1374.

See http://www.rsc.org/suppdata/dt/1999/1209/ for crystallographic files in .cif format.

## Results and discussion

The mechanism of action of platinum(IV) anticancer drugs appears first to involve reduction to the kinetically more labile platinum(II) analogue. Reduction of the antitumour agent *cis*,*trans*,*cis*-$[PtCl_2(OCOCH_3)_2(NH_3)(C_6H_{11}NH_2)]$ **2** is expected to give the cisplatin analogue *cis*-$[PtCl_2(NH_3)(C_6H_{11}NH_2)]$. As the aqueous solubility of the cyclohexylamine compounds is lower than that of the ammine derivatives and, as the latter are easier to prepare (especially as $^{15}N$ labelled materials for multinuclear NMR studies), we have synthesized *cis*,*trans*,*cis*-$[PtCl_2(OCOCH_3)_2(NH_3)_2]$ **1** as a simplified version of **2**. This has allowed us to study the reduction kinetics of **1** with the divalent sulfur amino acids L-$H_2$cys and L-Hmet as well as characterize the solid state structure of the complex. Incorporation of $^{15}NH_3$ permits multinuclear NMR investigation of reactions. The solubilities of **1** (18.3 mg cm$^{-3}$) and **2** (0.4 mg cm$^{-3}$) were determined, demonstrating the significant improvement in solubility on replacing the hydrophobic cyclohexylamine with ammine.

**Table 1** Selected bond lengths (Å) and angles (°) for *cis*,*trans*,*cis*-$[PtCl_2(OCOCH_3)_2(NH_3)_2]$ **1**

| | | | |
|---|---|---|---|
| Pt–O1 | 2.030(6) | C1–O1 | 1.303(11) |
| Pt–N1 | 2.049(6) | C1–O2 | 1.213(11) |
| Pt–Cl1 | 2.318(2) | C1–C2 | 1.502(14) |
| O1–Pt–O1A | 176.7(3) | N1–Pt–Cl1 | 177.1(2) |
| O1–Pt–N1 | 97.6(2) | N1–Pt–Cl1A | 89.1(2) |
| O1–Pt–N1A | 84.8(2) | N1–Pt–N1A | 90.7(4) |
| O1–Pt–Cl1 | 85.3(2) | Cl1–Pt–Cl1A | 91.23(10) |
| O1–Pt–Cl1A | 92.3(2) | | |

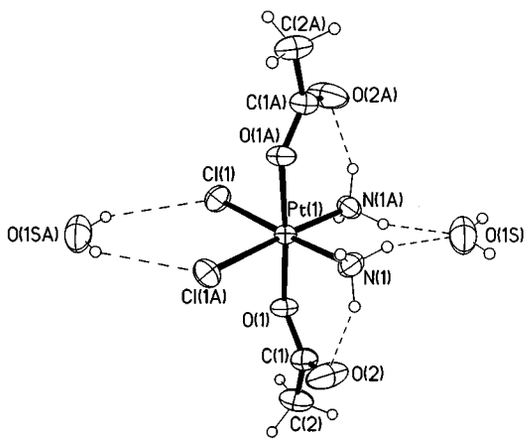


**Fig. 1** Molecular structure of complex **1** showing intra- and intermolecular hydrogen bonds.

### Crystal structure of *cis*,*trans*,*cis*-$[PtCl_2(OCOCH_3)_2(NH_3)_2]$ 1

A thermal ellipsoid diagram for complex **1** is shown in Fig. 1. Selected bond distance and angle data are given in Table 1. The co-ordination geometry about the $Pt^{IV}$ is octahedral. The two Cl atoms [Pt–Cl1 2.318(2) Å] and two ammine groups [Pt–N1 2.049(6) Å] are in a square-planar arrangement around the Pt atom similar to that of cisplatin.[14] The two acetato groups [Pt–O1 2.030(6) Å] are axial to this plane [O1–Pt–O1A 176.7(3)°]. Intramolecular hydrogen bonds between the ammine and non-co-ordinated carboxyl oxygen (N1 · · · O2 2.723 Å) and solvent water (N1 · · · O1S 2.894 Å) are observed. It is likely that in solution a solvent molecule is associated with the two ammine groups as observed in the solid state structure. The remaining ammine hydrogen has a very weak intermolecular interaction to a co-ordinated carboxylato O [N1 · · · O1 3.25 Å (N1: $x$, $1 - y$, $z - 0.5$)] and the water hydrogens have weak hydrogen-bonding interactions to the chloro moieties in an adjacent molecule [O1SA · · · Cl1 3.44 Å (O1SA: $x$, $y - 1$, $z$)]. Excluding the interactions to water, the hydrogen-bonding is very similar to that seen for *cis*,*trans*-$[Pt(en)Cl_2(OCOCH_3)_2]$[15] (where en is 1,2-diaminoethane) and $[Pt(en)(OCOCH_3)_2(cbdca)]$ (where $H_2$cbdca is cyclobutane-1,1-dicarboxylic acid).[16]

### Reactions of complex 1

**L-Cysteine.** A time-course series of $^1H$ NMR spectra of a solution of excess of L-$H_2$cys and complex **1** shows a decrease in the acetato singlet ($\delta$ 2.11) and L-$H_2$cys resonances with concomitant increases in free acetate ($\delta$ 1.90) and cystine. The

formation of free acetate shows the $Pt^{IV}$ has been reduced, the reductant being L-$H_2$cys as seen by the formation of cystine [$\delta$ 4.11(m), αH; 3.40(m), βH; 3.16(m), βH]. The $^{15}N$ NMR spectra (SUP 57512) of the reaction show a decrease in the peak from **1** ($\delta$ −41.74) and increase in a single resonance attributable to cisplatin ($\delta$ −68.62).[17] Accordingly, the reaction is formulated as in eqn. (1). Under the conditions of pseudo-first

$$\begin{aligned} &cis,trans,cis\text{-}[PtCl_2(OCOCH_3)_2(NH_3)_2] + \\ &\quad 2HSCH_2CH(NH_3^+)CO_2^- \longrightarrow cis\text{-}[PtCl_2(NH_3)_2] + \\ &\quad [-SCH_2CH(NH_3^+)CO_2^-]_2 + 2CH_3CO_2^- + 2H^+ \quad (1) \end{aligned}$$

order kinetics, excess of L-$H_2$cys is present and this then reacts further with the cisplatin produced. The $^{15}N$ NMR spectra of the reaction of $^{15}N$-**1** with $^{15}N$-L-$H_2$cys (1:5) were recorded. Initial resonances for free L-$H_2$cys and **1** present decreased with time and a small peak for cisplatin was detectable. After 24 h no cisplatin or platinum products were detectable in solution. Solid cystine had precipitated from solution, with the remaining L-$H_2$cys having formed oligomeric species, as described previously.[18] The resonance for $^{15}NH_4^+$ formed from released $^{15}NH_3$ overlapped with that of the reference.

**L-Methionine.** Reaction of complex **1** with L-Hmet (1:2) also produced free acetate and cisplatin as seen in the $^1H$ and $^{15}N$ NMR spectra respectively. The methyl singlet of L-Hmet was used as a convenient handle on the reaction progress as well as product identification. As the reaction proceeded resonances for free L-Hmet decreased [$\delta$ 2.12(s), $CH_3S$] with a concomitant increase in a new set of signals [$\delta$ 2.74 (s)]. Separate spectra of L-Hmet and L-methionine *S*-oxide were recorded which showed that methionine was consumed and the new sharp singlet observed is due to L-methionine *S*-oxide. The reaction is formulated as in eqn. (2).

$$\begin{aligned} &cis,trans,cis\text{-}[PtCl_2(OCOCH_3)_2(NH_3)_2] + \\ &\quad CH_3SCH_2CH_2CH(NH_3^+)CO_2^- + H_2O \longrightarrow \\ &cis\text{-}[PtCl_2(NH_3)_2] + CH_3S(O)CH_2CH_2CH(NH_3^+)CO_2^- + \\ &\quad 2CH_3CO_2^- + 2H^+ \quad (2) \end{aligned}$$

Incubation of complex **1** with excess of L-Hmet (1:4) for a week showed from $^{15}N$ NMR spectra that all cisplatin had reacted and new resonances were present. These have been assigned to *cis*-[Pt(L-met-*S*,*N*)$_2$] ($\delta$ −20.06, −20.24, −21.10) and *trans*-[Pt(L-met-*S*,*N*)$_2$] ($\delta$ −38.31, −38.60, −38.81).[17] A weak singlet at $\delta$ 18.64 is near to the resonance for free L-Hmet but could also be due to a monodentate S-only bonded species such as *cis*-[Pt(L-met-*S*,*N*)(L-met-*S*)$_2$]$^-$. The resonances from chelated L-Hmet typically appear in the same range as for *cis*-[Pt(L-met-*S*,*N*)$_2$] and would be obscured by these.

## Kinetics

Reduction of complex **1** was studied under pseudo-first-order conditions with L-$H_2$cys and L-Hmet in a 20-fold excess. $^1H$ NMR was used to monitor the decrease of the acetato singlet at $\delta$ 2.10 or the increase of free acetate at $\delta$ 1.90. A plot of ln $C_A$ or ln($C_A - C_Z$) against $t$ was linear (where $C_A$ is the peak intensity for bound and $C_Z$ free acetate) and the first-order rate constants can be obtained from the slope. The possibility of initial hydrolysis to give an activated aqua intermediate was ruled out by measuring the hydrolysis rate for **1**. After 20 d in 0.1 M deuteriated pH* 7.0 phosphate buffer no new peaks were observable by $^1H$ NMR.

The kinetic data were fitted assuming a mechanism whereby all protonation states of the reductant react in parallel, as suggested by Elding and co-workers[7,8] and depicted in Scheme 1. The observed rate constants, $k_{obs}$, are proportional to the excess concentration of reductant. Overall second-order kinetics are

**Table 2** Rate constants as a function of temperature and activation parameters for the reduction of *cis*,*cis*,*trans*-[$PtCl_2(OCOCH_3)_2(NH_3)_2$] **1** by L-cysteine and L-methionine at pH* 7.0

| | L-Cysteine[a] | L-Methionine |
|---|---|---|
| $k'$ (290 K) | $(2.9 \pm 0.4) \times 10^{-3}$ | — |
| $k'$ (295 K) | $(5.5 \pm 0.5) \times 10^{-3}$ | $(2.1 \pm 0.2) \times 10^{-6}$ |
| $k'$ (300 K) | $(7.0 \pm 0.4) \times 10^{-3}$ | $(3.9 \pm 0.1) \times 10^{-6}$ |
| $k'$ (305 K) | $(12.5 \pm 0.6) \times 10^{-3}$ | $(6.0 \pm 0.3) \times 10^{-6}$ |
| $k'$ (310 K) | — | $(11.1 \pm 0.4) \times 10^{-6}$ |
| $k_1$[b] | $(3.3 \pm 4.0) \times 10^{-4}$ | $(1.7 \pm 0.5) \times 10^{-6}$ |
| $k_2$ | $(2.9 \pm 1.8) \times 10^{-3}$ | $(3.4 \pm 0.3) \times 10^{-6}$ |
| $k_3$ | $(2.2 \pm 0.4) \times 10^{-2}$ | $(1.26 \pm 0.03) \times 10^{-5}$ |
| $k_4$ | $(6.2 \pm 0.3) \times 10^{-2}$ | — |
| $\Delta H^{\ddagger}$[c] | 65.7 ± 3.0 | 80.2 ± 2.7 |
| $\Delta S^{\ddagger}$[d] | −66.5 ± 2.5 | −83.2 ± 4.4 |

[a] $k'$/dm$^3$ mol$^{-1}$ s$^{-1}$. [b] $k_n$/dm$^3$ mol$^{-1}$ s$^{-1}$. [c] kJ mol$^{-1}$. [d] J K$^{-1}$ mol$^{-1}$.

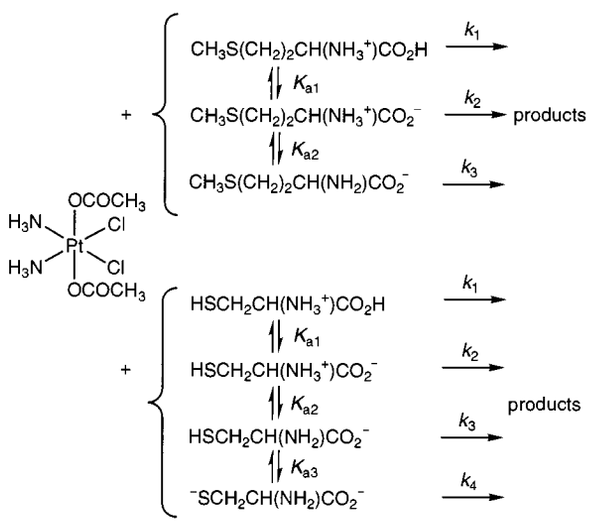


**Scheme 1**

observed according to eqn. (3), where $k'$ denotes the second-

$$\begin{aligned} &-d[PtCl_2(OCOCH_3)_2(NH_3)_2]/dt \\ &\quad = d[PtCl_2(NH_3)_2]/dt = d[CH_3CO_2^-]/2dt \\ &\quad = k'[\text{reductant}][PtCl_2(OCOCH_3)_2(NH_3)_2] \quad (3) \\ &\quad = k_{obs}\,[PtCl_2(OCOCH_3)_2(NH_3)_2] \end{aligned}$$

$$\text{where } k_{obs} = k'[\text{reductant}] \quad (4)$$

order rate constants for different reductants. Data were fitted ‡ using all $k_n$ and $K_{an}$ as variables and $k'$ are given in Table 2 along with the activation parameters, $\Delta H^{\ddagger}$ and $\Delta S^{\ddagger}$.

For both L-$H_2$cys and L-Hmet the rates increase as the pH increases, consistent with the deprotonated species being better reductants, Fig. 2. The fitted values for p$K_{an}$ derived from these plots agree well with the literature values (in parentheses):[19] L-$H_2$cys, p$K_{a1}$ 1.8 (1.9), p$K_{a2}$ 7.6 (8.1), p$K_{a3}$ 10.5 (10.1); L-Hmet, p$K_{a1}$ 2.5 (2.22), p$K_{a2}$ 8.5 (9.02). For L-$H_2$cys $k'$ is *ca.* 2000 times bigger than for L-Hmet, and may be attributable to the greater basicity of the thiol as compared to the thioether.[8] However, values of $k'$ are orders of magnitude lower for the

‡ Cysteine:

$$k' = \frac{k_1[H^+]^3 + k_2K_{a1}[H^+]^2 + k_3K_{a1}K_{a2}[H^+] + k_4K_{a1}K_{a2}K_{a3}}{[H^+]^3 + K_{a1}[H^+]^2 + K_{a1}K_{a2}[H^+] + K_{a1}K_{a2}K_{a3}}$$

Methionine:

$$k' = \frac{k_1[H^+]^2 + k_2K_{a1}[H^+] + k_3K_{a1}K_{a2}}{[H^+]^2 + K_{a1}[H^+] + K_{a1}K_{a2}}$$

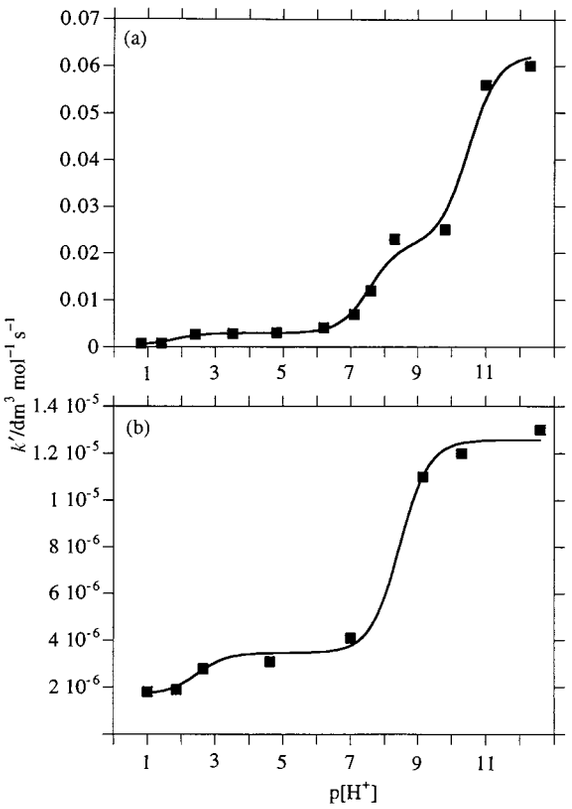


**Fig. 2** Plots of $k'$ *vs.* [H$^+$] for (a) L-cysteine and (b) L-methionine where the solid lines are those fitted using the equations in the text.

antitumour analogue **1** than for *trans*-$[Pt(CN)_4X_2]^{2-}$ (where X is $Cl^-$ or $Br^-$)[7,8] which was employed as a stable antitumour model complex. This has allowed us to determine all values of $k'$, which was not possible for *trans*-$[Pt(CN)_4X_2]^{2-}$ at higher pH values using stop-flow techniques, due to rapid reaction. The dramatically greater reactivity of *trans*-$[Pt(CN)_4X_2]^{2-}$ over **1** is a direct result of the in-plane cyano ligands which stabilize the platinum(II) oxidation state. As a measure of this we investigated the redox behaviour of complex **1** and *trans*-$[Pt(CN)_4X_2]^{2-}$. As is typical for platinum(IV) species, a reduction step is seen but the corresponding oxidation is not observed as reduction results in loss of the axial ligands. The cathodic potential for **1** of −689 mV is more negative than for $[Pt(en)Cl_2\{OC(O)R\}_2]$ (where R is alkyl)[15] which ranged from −493 to −546 mV and may be a reflection of the greater substitutional stability of the en chelate. All these complexes have significantly greater values than does *trans*-$[Pt(CN)_4X_2]^{2-}$ of −399 mV.

Our system is a close analogue to the drug JM216 (**2**) and affords a comparison of the kinetics expected for this. In biological media the major S-containing reductants are glutathione (γ-glutamylcysteinylglycine), L-$H_2$cys and L-Hmet. Given that glutathione and L-$H_2$cys have similar $k_n$ values for equivalent deprotonated species, the significantly greater rate of reduction of **1** by L-$H_2$cys and the typical concentrations of divalent sulfur compounds present in blood plasma and cells,[20] it is predicted that the predominant reductant will be glutathione > L-$H_2$cys > L-Hmet.

Platinum(IV) complexes prefer a low-spin, substitution-inert, $d^6$ octahedral geometry, so initial complex formation between reductant and $Pt^{IV}$ is highly unlikely. The reduction of $Pt^{IV}$ involves a two-electron transfer process and halide-mediated reductive-elimination reactions of platinum(IV)–halogen complexes involving various reductants have been suggested to take place *via* an attack by reductant on co-ordinated halide.[21] By analogy, the reductive elimination reaction of **1** may be interpreted in terms of oxygen-bridge electron transfer, with the transition state formulated as follows (where R = H, for L-$H_2$cys, $CH_3$ for L-Hmet).

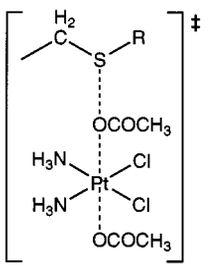


## Acknowledgements

Support for this work by the National University of Singapore (Grant RP 950651) and Miss Geok Kheng Tan for assistance with the crystal structure is greatly appreciated.

## References

1 K. M. Comess and S. J. Lippard, *Molecular Aspects of Anticancer Drug-DNA Interactions*, eds. S. Neidle and M. Waring, MacMillan, London, 1993, vol. 1, p. 134.
2 R. B. Weiss and M. C. Christian, *Drugs*, 1993, **46**, 360.
3 L. R. Kelland, B. A. Murrer, G. Abel, C. M. Giandomenico, P. Mistry and K. R. Harrap, *Cancer Res.*, 1992, **52**, 822.
4 R. M. Roat and J. Reedijk, *J. Inorg. Biochem.*, 1993, **52**, 263.
5 F. I. Raynaud, D. E. Odell and L. R. Kelland, *Br. J. Cancer*, 1996, **74**, 380.
6 G. R. Gibbons, S. D. Wyrick and S. G. Chaney, *Cancer Res.*, 1989, **49**, 1402; M. Laverick, A. H. W. Nias, P. J. Sadler and I. M. Ismail, *Br. J. Cancer*, 1981, **43**, 732; J. L. Van der Veer, A. R. Peters and J. Reedijk, *J. Inorg. Biochem.*, 1986, **26**, 137.
7 T. S. Shi, J. Berglund and L. I. Elding, *Inorg. Chem.*, 1996, **35**, 3498.
8 T. S. Shi, J. Berglund and L. I. Elding, *J. Chem. Soc.*, *Dalton Trans.*, 1997, 2073.
9 S. Dhara, *Indian J. Chem.*, 1970, **8**, 193.
10 A. V. Babaeva, *Dokl. Akad. Nauk SSSR*, 1939, **23**, 653.
11 *SMART & SAINT Software Reference Manuals*, Version 4.0, Siemens Energy & Automation, Inc., Analytical Instrumentation, Madison, WI, 1996.
12 G. M. Sheldrick, SADABS, software for empirical absorption correction, University of Göttingen, 1996.
13 *SHELXTL Reference Manual*, Version 5.03, Siemens Energy & Automation, Inc., Analytical Instrumentation, Madison, WI, 1996.
14 G. H. W. Milburn and M. R. Truter, *J. Chem. Soc. A*, 1966, 1609.
15 L. T. Ellis, H. M. Er and T. W. Hambley, *Aust. J. Chem.*, 1995, **48**, 793.
16 Y. Deng and A. R. Khokar, *Inorg. Chim. Acta*, 1993, **204**, 35.
17 R. E. Norman, J. D. Ranford and P. J. Sadler, *Inorg. Chem.*, 1992, **31**, 877.
18 R. N. Bose, S. K. Ghosh and S. Moghaddas, *J. Inorg. Biochem.*, 1997, **65**, 199.
19 R. M. Smith and A. E. Martell, *Critical Stability Constants*, Plenum, New York, 1989, vol. 6, suppl. 2, pp. 20–24.
20 H. C Potgieter, J. B. Ubbink, S. Bissbort, M. J. Bester, J. H. Spies and W. J. H. Vermaak, *Anal. Biochem.*, 1997, **248**, 86; A. Pastore, R. Massoud, C. Motti, A. Lo Russo, G. Fucci, C. Cortese and G. Federici, *Clin. Chem.*, 1998, **44**, 825.
21 J. Berglund, R. Voigt, S. Fronaeus and L. I. Elding, *Inorg. Chem.*, 1994, **33**, 3346; P. Chandayot and Y.-T. Fanchiang, *Inorg. Chem.*, 1985, **24**, 3532, 3535.

*Paper 9/00441F*